A&A 508, 201–207 (2009)
DOI: 10.1051/0004-6361/200912658

Astronomy & Astrophysics

The HI properties of galaxies in the Coma I cloud revisited *(Research Note)*

A. Boselli[1] and G. Gavazzi[2]

[1] Laboratoire d'Astrophysique de Marseille, UMR 6110 CNRS, 38 rue F. Joliot-Curie, 13388 Marseille, France
e-mail: Alessandro.Boselli@oamp.fr
[2] Universita degli Studi di Milano-Bicocca, Piazza delle Scienze 3, 20126 Milano, Italy
e-mail: Giuseppe.Gavazzi@mib.infn.it

Received 9 June 2009 / Accepted 19 September 2009

ABSTRACT

Context. Pre-processing within small groups has been proposed to explain several of the properties of galaxies lying in rich clusters.
Aims. The aim of the present work is to see whether pre-processing is acting in the nearby universe, where the structures that are merging to form rich clusters are large and massive.
Methods. We study the HI gas properties of a large sample of late-type galaxies belonging to the Coma I cloud, an association of objects close to the Virgo cluster.
Results. Contrary to what was previously claimed, late-type galaxies in the Coma I cloud are not deficient in HI gas (HI – def = 0.06 ± 0.44).
Conclusions. If the Coma I cloud is representative of infalling groups in nearby clusters, this result suggests that, in the local universe, the evolution of late-type galaxies belonging to loose structures with high velocity dispersions ($\geq$300 km s^{-1}) associated with rich clusters such as Virgo is not significantly perturbed by pre-processing.

Key words. galaxies: general – galaxies: ISM – galaxies: distances and redshifts – galaxies: clusters: general

1. Introduction

The morphology segregation effect (Dressler 1980; Whitemore & Gilmore 1991) is the strongest evidence that the environment plays a major role in shaping galaxy evolution. Recent surveys such as SDSS (Gomez et al. 2003) and 2dF (Lewis et al. 2002), which have allowed us to continuously trace galaxy properties from the highest density regions in the core of rich clusters down to the field, have shown that the star formation activity decreases at the periphery of clusters, probably because the interactions responsible for removal of gas, the principal feeder of star formation (e.g. Boselli et al. 2001), were already in place in the infalling groups prior to the formation of rich clusters. These results are consistent with our own studies of the gas and star formation properties of galaxies in nearby clusters (Gavazzi et al. 2002, 2005, 2006a,b, 2008). Although in some cases the presence of hot gas might trigger galaxy interactions with the intergalactic medium, the low velocity dispersion of small groups ($\leq$200 km s^{-1}) suggests that gravitational interactions are probably at the origin of the pre-processing of galaxies even before they enter rich clusters (Dressler 2004).

Pre-processing is probably efficient at high redshift, when clusters are under formation (Gnedin 2003). Pre-processing is less evident in the nearby universe (Boselli & Gavazzi 2006), where clusters are rather accreting large structures characterized by high velocity dispersions (Donnelly et al. 2001; Ferrari et al. 2003; Cortese et al. 2004) or single galaxies, making gravitational interactions rather rare. For instance, the velocity dispersion of the M and W clouds in the Virgo cluster are relatively high, of the order of 450–650 km s^{-1} (Gavazzi et al. 1999), thus almost comparable to that of an already formed cluster. The only exception found in the local universe is the blue infalling group in A1367 (Sakai et al. 2002; Gavazzi et al. 2003a; Cortese et al. 2006), a compact group of galaxies with a velocity dispersion of only 150 km s^{-1} falling into the cluster A1367. Here pre-processing is efficiently perturbing the galaxy morphology and star formation activity, creating long tails of ionized gas.

The study of the Virgo cluster, the nearest rich cluster of galaxies, and its surroundings, however, revealed the presence of satellite clouds with HI-deficient objects revealing an ongoing interaction, thus making these clouds of particular interest in studying pre-processing in the nearby universe. Being loosely anchored to the galaxy potential, the HI component can be easily removed during any kind of interaction, and is thus an ideal tracer of ongoing perturbations (Boselli & Gavazzi 2006). Among these, the Coma I cloud, a loose aggregation of galaxies in the projected direction of the Coma/A1367 supercluster located at ~5 Mpc from M 87 (see Sects. 4 and 5), is the most promising target since previous studies have shown that this loose cloud is composed of HI-deficient galaxies (Garcia-Barreto et al. 1994). The availability of new HI data more than doubled the sample of Garcia-Barreto et al. (1994), suggesting the importance of reanalyzing the HI gas properties of the Coma I cloud galaxies in the framework of pre-processing in the nearby universe.

2. The sample

The Coma I cloud has been defined by Gregory & Thompson (1977) as the cloud of nearby galaxies ($\leq$20 Mpc) in the foreground of the Coma/A1367 supercluster. The analysis presented in this work is thus based on a sample composed of all

galaxies extracted from NED in the sky region $11^h30^m < RA (2000) < 13^h30^m$; $20^o < Dec < 34^o$ with a recessional velocity $\leq$2000 km s^{-1}. Excluding misclassified HII regions associated with bright galaxies, the resulting sample is composed of 161 galaxies. Since no limits on the magnitude or diameter of the selected galaxies are applied, the selected sample is not complete in any sense.

3. The data

The set of data necessary for the following analysis, restricted to those galaxies with available HI data (72 objects), are listed in Table 1. This includes morphological type, optical and near IR magnitudes, optical diameters and HI flux and line width measurements. Coordinates and morphological type have been taken from NED, in its updated version including the SDSS data release 6. For galaxies without a morphological classification, we assigned a morphology type according to, in order of preference, the presence of emission lines in the SDSS spectra, their optical color on the SDSS composed image or their optical appearance on the POSS plates. Thanks to their proximity, the morphological classification of the brightest galaxies, those with available HI data and thus the most concerned by the present analysis, is very accurate, to less than one bin in the Hubble sequence. It is poor for the very compact sources that dominate at low luminosity. The discrimination between early and late-type galaxies, based on spectroscopic measurements or optical colors, however, should be reliable.

Optical diameters have been taken from GOLDMine (Gavazzi et al. 2003b) whenever available, or from NED otherwise. We preferred to use the GOLDMine values whenever possible to be as consistent as possible in the definition and in the determination of the HI-deficiency parameter, which here is based on the calibrations of Solanes et al. (1996). Near infrared *JHK* total magnitudes have been taken from 2MASS (Jarrett et al. 2003) whenever available, or from Gavazzi & Boselli (1996). The comparison of 2MASS and GOLDMine total magnitudes that we made using an extended sample indicates that they differ by less than 0.1 mag.

HI data have been taken from several sources in the literature: to be consistent with the distance determination using the Tully-Fisher calibration given by Masters et al. (2008), HI fluxes and velocity widths have been taken whenever available from Springob et al. (2005). These data also have the advantage of being accurately homogenized. HI line widths from other sources have been corrected for smoothing, redshift stretch and turbulent motion (6.5 km s^{-1}) as described in Springob et al. (2005). HI fluxes of sources others than Springob et al. (2005) have been corrected consistently for pointing offsets and beam attenuation. The accuracy in the fluxes should be of the order of 10–15% (Springob et al. 2005), and of the order of 10 km s^{-1} in the line width measurements.
Galaxies in Table 1 are arranged as follow:

- Column 1: galaxy name. Column 2: morphological type, from NED whenever available, or from our own classification;
- Column 3 and 4: major and minor optical diameters, from GOLDMine whenever available, from NED elsewhere. These are B band isophotal diameters at the 25 mag arcsec^{-2};
- Column 5: optical (generally B band (m_B)) magnitude, from NED;
- Column 6: heliocentric velocity, in km s^{-1}, from NED;
- Column 7: Tully-Fisher distance, in Mpc, determined as explained in Sect. 4.2. Distances for those galaxies with available primary indicators are taken from Ferrarese et al. (2000). For galaxies without a direct distance estimate, we assume 14.52 Mpc;
- Column 8: Coma I cloud (CI) members and background (Bg) objects, whose identification has been determined as explained in Sect. 4.1;
- Column 9: HI flux, in Jy km s^{-1} corrected for pointing offset and beam attenuation consistent with Springob et al. (2005);
- Column 10: HI line width at 50%, defined as in Springob et al. (2005; W_{F50}), corrected for smoothing, redshift stretch and turbulent motion as prescribed by Springob et al. (2005);
- Column 11: logarithm of the HI mass, in solar units;
- Column 12: reference to the HI data;
- Column 13: the HI deficiency parameter, determined as described in the text;
- Column 14: a code for the HI line profile, from Springob et al. (2005) whenever available, or with the following criteria: 1 for high signal to noise two horn profiles; 2 for high signal to noise one horn profiles; 3 for fair profiles; 4 for low signal to noise, bad quality profiles and 5 for unavailable profiles.

4. The derived parameters

4.1. Cloud membership

The distribution on the sky and in the velocity space of the selected galaxies is shown in Fig. 1. The wedge diagram shown in the lower panel clearly indicates that the Coma I cloud is confined within recessional velocities $\leq$1500 km s^{-1}. To avoid any possible contamination from unclassified objects possibly associated to our galaxy, we arbitrarily remove any object with recessional velocity <100 km s^{-1} (none of these objects have HI data).

The average recessional velocity of the galaxies identified as Coma I cloud members (132 objects in the $100 \leq vel_{hel} \leq 1500$ km s^{-1}) is $vel_{hel} = 773 \pm 307$ km s^{-1}. The velocity dispersion is relatively small for a structure extended over ~250 square degrees, in particular if compared to that observed in the W and M clouds (see Table 2) located in the background of the Virgo cluster, at ~32 Mpc (Gavazzi et al. 1999).

As defined, the Coma I cloud is an aggregation of objects with a spiral fraction of 68%, thus slightly higher than the W (54%) and M (62%) clouds in the Virgo cluster. An overdense region is visible around NGC 4278 (ρ_{xyz} = 1.25 galaxies/Mpc^3, where ρ_{xyz} is the local density of galaxies brighter than $M_B = -16$, in galaxies/Mpc^3, within a three-dimensional grid 0.5 Mpc wide; Tully 1988b): this density is slightly lower than that observed in the periphery of the Virgo cluster ($\rho_{xyz} \sim 1.4$ galaxies/Mpc^3; Tully 1988a).

4.2. Distance determination

An accurate determination of the gas properties of the target galaxies needs a precise distance determination. Five galaxies in the studied region have distance measurements from primary indicators such as cepheids (NGC 4414, NGC 4725), planetary nebulae and globular cluster luminosity functions (NGC 4278, NGC 4494, NGC 4565) and surface brightness fluctuations (NGC 4278, NGC 4494, NGC 4565, NGC 4725) (Ferrarese et al. 2000).

For inclined galaxies (inclination $\geq$30 deg) with available HI line widths and *JHK* total magnitudes, the distance can be inferred using the Tully-Fisher relation determined adopting the

Table 1. Galaxies with HI data.

Name	Type	a '	b '	Mag	Vel km s^{-1}	Dist Mpc	Memb	SHI Jy km s^{-1}	WHIc km s^{-1}	MHI $M_\odot$	Ref.[a]	HI–def	Wqual
NGC 3712	SB?	1.70	0.60	14.90	1580	–	Bg	7.60	119	9.04	4	–0.07	1
UGC 6599	Ibm	1.20	0.70	16.50	1569	–	Bg	5.31	104	8.88	2	–0.12	5
UGC 6610	Scd:	2.10	0.40	15.00	1851	–	Bg	12.76	199	9.39	1	–0.20	1
UGC 6637	S0	0.90	0.46	15.00	1836	–	Bg	1.84	132	8.54	15	–0.11	5
UGC 6684	IA?(s)mV:	1.00	0.40	15.70	1788	–	Bg	5.78	124	9.02	2	–0.30	1
IC2957	S0-a	0.60	0.40	14.80	1776	8.6	Bg	2.24	88	8.60	1	–0.51	3
UGC 6782	ImV	2.00	2.00	15.00	525	–	CI	6.96	83	8.54	1	0.21	1
NGC 3900	SA(r)0+	3.16	1.70	12.50	1798	–	Bg	16.84	420	9.48	1	–0.10	1
UGC 6791	Scd:	2.05	1.41	14.99	1852	29.3	Bg	5.10	212	8.99	1	0.18	1
NGC 3899	SAB(s)b?pec	2.45	1.07	13.21	1779	10.4	Bg	4.87	159	8.94	2	0.24	2
UGC 6881	Im:	1.40	0.70	17.00	607	–	CI	2.42	66	8.08	2	0.45	2
UGC 6900	Sd	2.00	1.29	14.80	590	–	CI	1.69	83	7.92	2	0.82	1
NGC 4020	Sbd?sp	2.00	0.73	13.28	760	14.2	CI	14.64	161	8.84	1	–0.11	1
CGCG157080	Irr	0.58	0.42	15.00	714	–	CI	2.64	125	8.12	3	–0.12	2
NGC 4032	Im:	1.90	1.80	12.81	1268	–	CI	22.10	94	9.04	5	–0.33	2
UGC 7007	SB(s)mIV	0.84	0.79	15.50	774	–	CI	2.90	36	8.16	2	0.06	2
NGC 4062	SA(s)c	1.59	1.16	12.50	769	25.5	CI	24.13	293	9.57	1	–0.54	1
NGC 4080	Im?	1.20	0.50	14.28	567	10.9	CI	2.86	138	7.90	2	0.36	1
IC2992	S0?	0.60	0.60	14.80	580	–	CI	1.42	–	7.85	15	–0.25	5
UGC 7131	Sdm:	1.50	0.40	15.10	253	–	CI	4.56	100	8.35	2	0.22	1
NGC 4136	SAB(r)c	4.00	3.70	11.69	609	–	CI	39.51	84	9.29	6	0.00	1
NGC 4173	Sdm:	5.04	0.69	13.59	1127	–	CI	42.12	75	9.32	7	–0.01	1
UGC 7236	Im:	1.10	0.90	16.28	945	–	CI	4.75	57	8.37	8	0.01	4
NGC 4203	SAB0-	3.40	3.20	11.80	1086	–	CI	48.11	234	9.38	9	–0.44	1
NGC 4204	SB(s)dm	3.60	2.90	12.90	856	–	CI	34.28	65	9.23	7	–0.13	1
MRK1315	BCD	1.05	0.60	16.50	847	–	CI	20.89	-	9.02	15	–0.66	5
UGC 7300	Im	1.40	1.20	14.90	1210	–	CI	14.51	77	8.86	1	–0.33	1
UGC 7321	Sd	6.74	0.43	14.00	408	21.7	CI	44.51	217	9.69	1	0.04	1
NGC 4245	SB(r)0/a:	2.90	2.20	12.31	815	15.3	CI	0.76	214	7.62	1	1.23	1
NGC 4274	(R)SB(r)ab	6.80	2.50	11.34	930	17.1	CI	9.91	432	8.83	10	0.72	1
NGC 4278	E1-2	4.10	3.80	11.20	649	12.6[b]	CI	10.52	395	8.59	16	0.38	2
NGC 4286	SA(r)0/a:	1.60	1.00	14.10	644	–	CI	0.71	–	7.55	15	0.81	5
UGC 7428	Im:	1.30	1.20	14.10	1137	–	CI	7.35	49	8.56	2	–0.08	2
IC3215	Sdm:	1.26	0.35	15.00	1019	–	CI	2.64	102	8.12	2	0.35	2
NGC 4310	(R')SAB(r)0+?	2.20	1.20	13.22	913	10.4	CI	1.15	166	7.47	11	0.88	2
NGC 4314	SB(rs)a	4.20	3.70	11.43	963	–	CI	0.40	111	7.30	1	1.92	1
IC3247	Sd	1.86	0.26	15.25	569	23.0	CI	3.50	152	8.64	1	0.34	1
NGC 4359	SB(rs)c?sp	3.50	0.80	13.40	1253	–	CI	14.72	–	8.86	15	0.33	0
IC3308	Sdm:	1.30	0.20	15.41	316	–	CI	13.30	131	8.82	3	–0.34	2
NGC 4395	SA(s)m:	13.20	11.00	10.64	319	13.9	CI	401.61	117	10.26	1	–0.40	1
NGC 4393	SABd	3.20	3.00	12.70	755	–	CI	25.35	92	9.10	15	–0.07	5
NGC 4414	SA(rs)c?	3.60	2.00	10.96	716	19.1[b]	CI	70.20	347	9.78	1	–0.36	1
UGC 7584	Sdm:	0.90	0.50	16.00	603	–	CI	3.65	33	8.26	1	0.00	1
NGC 4448	SB(r)ab	3.90	1.40	12.00	661	18.4	CI	3.00	377	8.38	1	0.93	1
NGC 4455	SB(s)d?sp	2.80	0.80	12.93	637	–	CI	30.67	98	9.18	1	–0.23	1
UGC 7673	ImIII-IV	1.40	1.30	15.28	642	–	CI	10.38	73	8.71	1	–0.18	1
UGC 7698	Im	6.50	4.50	13.00	331	–	CI	40.98	59	9.31	1	0.15	1
NGC 4509	Sab pec?	0.90	0.60	14.10	937	6.1	CI	6.49	57	7.81	9	0.21	2
NGC 4525	Scd:	2.37	0.96	13.40	1172	9.2	CI	9.94	141	8.29	1	0.28	1
NGC 4562	SB(s)dm:sp	2.32	0.69	13.90	1353	–	CI	8.29	121	8.61	1	0.22	1
NGC 4559	SAB(rs)cd	10.70	4.40	10.46	816	7.2	CI	340.70	236	9.62	1	–0.28	1
IC3571	BCD	0.60	0.50	17.79	1260	–	CI	0.91	–	7.65	17	0.36	5
NGC 4565	SA(s)b?sp	15.90	1.85	10.42	1230	13.4[b]	CI	341.11	394	10.16	1	–0.12	3
UGC A292	ImIV-V	1.00	0.70	16.00	308	–	CI	15.64	28	8.89	1	–0.57	1
NGC 4631	SB(s)d	15.50	2.70	9.75	606	5.3	CI	1077.60	276	9.86	12	–0.48	1
MCG+06-28-022	BCD	0.68	0.58	15.40	892	–	CI	1.42	–	7.85	15	0.24	5
NGC 4656	SB(s)m pec	6.46	0.66	10.60	664	–	CI	190.55	–	9.98	15	–0.52	5
UGC A294	S0 pec	0.70	0.40	15.10	947	–	CI	6.89	84	8.53	3	–0.82	2
NGC 4670	SB(s)0/a pec:BCD	1.40	1.10	13.09	1069	20.9	CI	15.35	121	8.88	13	–0.35	1
UGC A298	BCD?	0.50	0.30	15.50	801	1.9	CI	0.73	38	7.56	14	0.34	2
NGC 4725	SAB(r)ab pec	10.70	7.60	10.11	1206	13.0[b]	CI	141.19	382	9.75	1	–0.10	1
UGC 7990	Im	1.00	0.60	17.00	512	–	CI	2.38	70	8.07	2	0.25	1
KUG1249+263	Irr	0.60	0.40	16.72	1225	–	CI	2.33	–	8.06	15	–0.05	5
NGC 4747	Sbcd? pec sp	3.50	1.20	12.96	1190	10.7	CI	39.00	155	9.02	8	–0.12	3
IC3840	Sm/Irr:	1.00	0.24	16.90	583	–	CI	2.23	–	8.04	15	0.28	5
UGC 8011	Im	1.40	1.10	18.00	776	–	CI	10.18	116	8.70	1	–0.17	1
MRK1338	E	0.40	0.20	15.50	1069	–	CI	0.68	19	7.53	14	–0.24	2
NGC 4789A	IB(s)mIV-V	3.00	2.20	13.94	374	19.7	CI	31.77	70	9.46	1	–0.28	1
UGC 8030	Im:	0.83	0.44	18.00	628	–	CI	1.36	34	7.83	15	0.38	2
NGC 4826	(R)SA(rs)ab	10.00	5.40	9.36	408	4.9	CI	51.25	308	8.47	1	0.65	1
UGC 8181	Sdm:	1.50	0.40	16.00	886	–	CI	3.99	80	8.30	2	0.27	1
UGC 8333	Im:	1.30	0.40	17.00	935	–	CI	11.88	125	8.77	1	–0.29	1

Notes: *a*: references to HI data: 1 = Springob et al. 2005; 2 = Schneider et al. (1990); 3 = Scodeggio & Gavazzi (1993); 4 = Theureau et al. (1998); 5 = Helou et al. (1984); 6 = Lewis (1987); 7 = Fisher & Tully (1981); 8 = Huchtmeier & Richter (1989); 9 = Noordermeer et al. (2005); 10 = Huchtmeier (1982); 11 = Chamaraux et al. (1987); 12 = Rots (1980); 13 = Thuan (1981); 14 = Huchtmeier et al. (2005); 15 = Hyperleda; 16 = Burstein et al. (1987); 17 = Dahlem et al. (2005)
b: from Ferrarese et al. (2000).

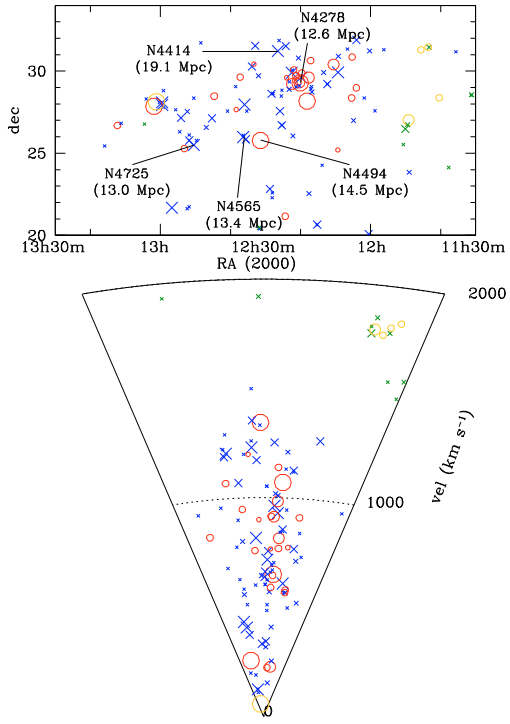

Fig. 1. The sky distribution (*upper panel*) and the wedge diagram (*lower panel*) of galaxies in the studied region. Red circles are for early-type (≤S0a), blue crosses for late-type galaxies in the Coma I cloud region as defined in the text, orange circles and green crosses for early- and late-type galaxies in the background (vel_{hel} > 1500 km s^{-1}) or in the foreground (vel_{hel} < 100 km s^{-1}). The size of the symbols decreases from bright (m_{pg} < 12 mag) to weak (m_{pg} ≥ 16 mag) sources, in 2 mag bin intervals.

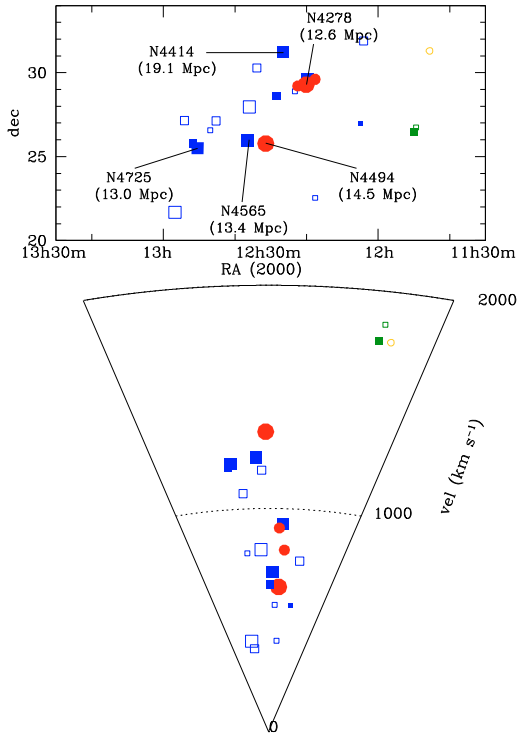

Fig. 2. Same as Fig. 1: filled symbols are for galaxies with a distance within 5 Mpc of the average distance of the Coma I cloud as determined from primary indicators (14.52 ± 5 Mpc), empty symbols for galaxies outside this distance range. Red circles are for early-type (≤S0a), blue squares for late-type galaxies in the Coma I cloud, orange circles and green squares for early- and late-type galaxies in the background (vel_{hel} > 1500 km s^{-1}) or in the foreground (vel_{hel} < 100 km s^{-1}). The size of the symbols decreases from bright (m_{pg} < 12 mag) to weak (m_{pg} ≥ 16 mag) sources, in 2 mag bin intervals.

Table 2. Coma I and Virgo clouds properties.

Cloud	N.[a]	Extension	S%[b]	σ_{vel}(km s^{-1})	HI-def
Coma I	115(55)	~250^{o2}	68	307	0.06 ± 0.44
Virgo W	173(37)	~12^{o2}	54	437[c]	0.63 ± 0.68
Virgo M	39(23)	~4^{o2}	62	666[c]	0.24 ± 0.57

Notes: [a]: number of cataloged objects to mag ≤18; the number in parenthesis gives the late-type objects with HI data.
[b]: spiral fraction to $M_B \leq -15$.
[c]: from Gavazzi et al. (1999).

Masters et al. (2008) calibration. For these 27 galaxies, we estimate their distance as the average of the *JHK* Tully-Fisher distance. We notice that for the three galaxies having both distance estimates, the Tully-Fisher distance is systematically lower than that obtained from the primary indicators by ~3.5 Mpc.

The average distance of the Coma I cloud members defined in the previous section[1] is 13.91 ± 5.72 Mpc, while it is 14.52 ± 2.66 Mpc considering only the five galaxies with primary distance indicators. In the following analysis we assume a distance of 14.52 Mpc for those galaxies belonging to the Coma I cloud without any direct distance measurement. For the few background galaxies (vel_{hel} ≥ 1500 km s^{-1}) the distance is determined assuming a Hubble constant of H_0 = 73 km s^{-1} Mpc^{-1} once their recessional velocity is corrected for a Virgocluster infall of 224 km s^{-1}.

[1] For galaxies with both primary distance indicators and Tully-Fisher distances, the former are adopted.

4.3. The gas mass and the HI-deficiency parameter

The HI gas mass has been determined using the relation:

$$\mathrm{MHI} = 2.36 \times 10^5 \mathrm{SHI(Jy\,km\,s^{-1})Dist^2(Mpc)} \quad (1)$$

where the distance is determined as described in the previous section.

The HI-deficiency parameter (HI−def) is defined as the logarithmic difference between the average HI mass of a reference sample of isolated galaxies of similar type and linear dimension and the HI mass actually observed in individual objects: HI−def = log MHI$_{ref}$ − log MHI$_{obs}$. According to Haynes & Giovanelli (1984), log h^2MHI$_{ref}$ = c + d log(hdiam)^2, where c and d are weak functions of the Hubble type, diam is the linear diameter of the galaxy (see Gavazzi et al. 2005) and $h = H_0/100$. In the present analysis we use the calibration of Solanes et al. (1996) for late-type galaxies, extended to Scd-Im-BCD objects as prescribed in Gavazzi et al. (in preparation) (see Table 3). This calibration is based on a sample of 98 galaxies of type ≥ Scd in the local supercluster (excluding the Virgo cluster), observed by ALFALFA in the sky region 11^h < RA(2000) < 16^h, 4^o < Dec < 16^o and in the velocity range 0 < vel_{hel} < 2000 km s^{-1} and is, at present, the best available calibration for this morphological class. It is preferred to the highly uncertain calibration of Haynes & Giovanelli (1984) which is based on a small sample of 38 Scd-Im-BCD galaxies mostly of large diameter (Gavazzi et al. 2008; Solanes et al. 1996).

The average HI deficiency of galaxies in the Coma I cloud is HI−def = 0.06 ± 0.44, thus slightly higher than the average

Table 3. The calibration of the HI deficiency parameter.

Type	c	d	Ref.
E-S0a	6.88	0.89	HG84
Sa-Sab	7.75	0.59	S96
Sb	7.82	0.62	S96
Sbc	7.84	0.61	S96
Sc	7.16	0.87	S96
Scd-Im-BCD	7.45	0.70	G10

References: HG84: Haynes & Giovanelli (1984); S96: Solanes et al. (1996); G10: Gavazzi et al. (in preparation).

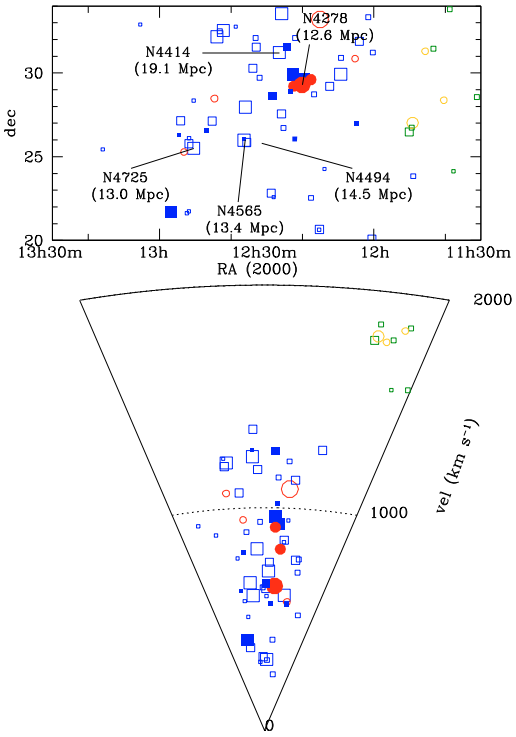

Fig. 3. Same as Fig. 1: filled symbols are for HI-deficient galaxies (HI − def > 0.3), empty symbols for galaxies with a normal HI content (HI − def ≤ 0.3). Red circles are for early-type (≤S0a), blue squares for late-type galaxies in the Coma I cloud region as defined in the text, orange circles and green squares for early- and late-type galaxies in the background (vel_{hel} > 1500 km s^{-1}) or in the foreground (vel_{hel} < 100 km s^{-1}). The size of the symbols decreases from bright (m_{pg} < 12 mag) to weak (m_{pg} ≥ 16 mag) sources, in 2 mag bin intervals.

value for unperturbed field objects (HI − def = 0.00 ± 0.30; Haynes & Giovanelli 1984). This result is robust against the adopted calibration of the HI-deficiency parameter since it does not change significantly using the c = 7.00 and d = 0.94 coefficients for Scd-Im-BCD galaxies of Haynes & Giovanelli (1984): HI − def = 0.03 ± 0.44, thus consistent with our estimate. Out of the 55 late-type Coma I cloud members with available HI data, only 13 (24%) can be considered as deficient in HI gas with HI deficiencies greater than 0.3. These most deficient objects (filled squares in Fig. 3) do not seem to be located in particular zones of the sky or of the velocity space, nor are objects at the average distance of the Coma I cloud but with high velocity with respect to the cloud (Fig. 4).

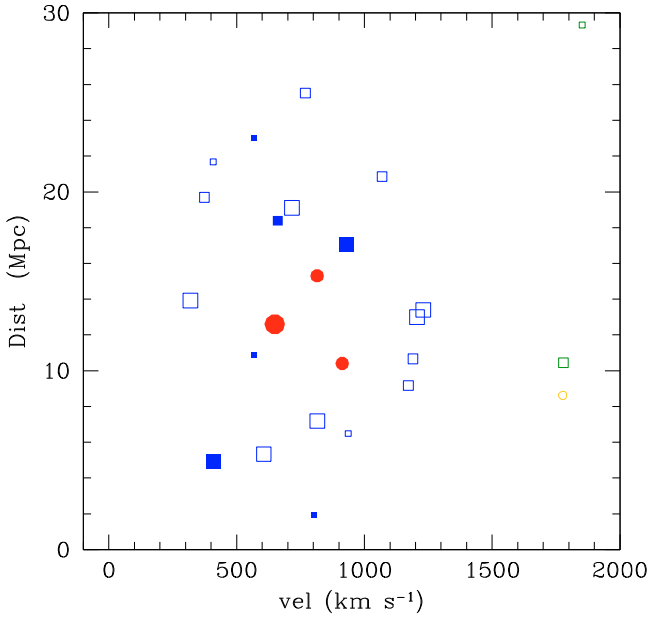

Fig. 4. The distance-velocity diagram of galaxies in the studied region. Filled symbols are for HI-deficient galaxies (HI − def > 0.3), empty symbols for galaxies with a normal HI content (HI − def ≤ 0.3). Red circles are for early-type (≤S0a), blue squares for late-type galaxies in the Coma I cloud region as defined in the text, orange circles and green squares for early- and late-type galaxies in the background (vel_{hel} > 1500 km s^{-1}) or in the foreground (vel_{hel} < 100 km s^{-1}). The size of the symbols decreases from bright (m_{pg} < 12 mag) to weak (m_{pg} ≥ 16 mag) sources, in 2 mag bin intervals.

5. Discussion and conclusion

By studying the HI properties of 32 galaxies in the Coma I cloud with data taken at Effelsberg, Garcia-Barreto et al. (1994) concluded that these objects are generally devoid of gas. In their sample of 23 late-type galaxies the average HI-deficiency is 0.40 ± 0.59, significantly higher than the value found in this work (HI − def = 0.06 ± 0.44) on a sample more than doubled in size (55 objects). The difference with Garcia-Barreto et al. (1994) might result from several reasons. The HI fluxes used in this work, mostly (64%) taken from the compilation of Springob et al. (2005), are systematically higher (22%) than those of Garcia-Barreto et al. (1994) (see Fig. 5). The resulting HI-deficiency parameter is thus lower by a factor of 0.09 on average than the previous estimate. This difference can be due to the fact that Springob et al. (2005) correct the data for beam attenuation and pointing offsets, while it is unclear whether Garcia-Barreto et al. (1994) used similar corrections. An additional difference of 0.03 in HI − def is due to the fact that, to transform SHI fluxes into gas masses, Garcia-Barreto et al. (1994) in Eq. (1) used a constant value of 2.22×10^5 instead of 2.36×10^5 as in this work. The relationship between optical linear diameters and the HI mass being non linear, the HI-deficiency parameter is not a distance independent value: for a given galaxy the HI-deficiency increases if its distance decreases. Garcia-Barreto et al. (1994) used a distance of 10 Mpc in the determination of the HI mass of their sample, while we used the Tully-Fisher distance whenever available, or 14.52 Mpc elsewhere. This difference in distance leads to an overestimate of the HI-deficiency parameter of ∼0.04 for a typical Sc galaxy in the Garcia-Barreto et al. calculations with respect to ours. Conversely, the use of the calibration of Solanes et al. (1996) for Sa-Sc galaxies, which

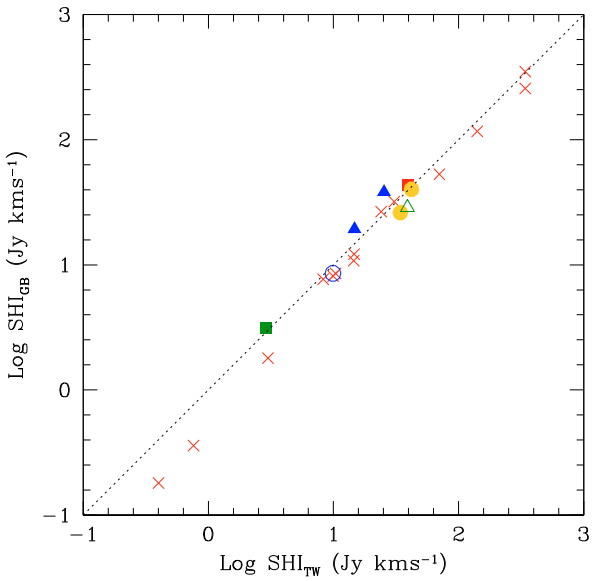

Fig. 5. Comparison of the HI fluxes (in Jy km s^{-1}) used in this work to those determined from Table 1 of Garcia-Barreto et al. (1994) using a distance of 10 Mpc and the relation given in Eq. (1). Red crosses indicates data from Springob et al. (2005), red filled squares from Lewis (1987), blue filled triangles from HyperLeda, green filled squares from Schneider et al. (1990), orange filled dots from Fisher & Tully (1981), blue empty dots from Huchtmeier (1982) and green empty triangles from Huchtmeier & Richter (1989). The dotted line shows the one to one relation.

is based on $H_0 = 100$ km s^{-1} Mpc^{-1}, induces a decrease of the HI-deficiency parameter by a factor $(1-d)\mathrm{Log}\,h^2$ (from 0.11 for Sa to 0.04 for Sc). Since the present sample is dominated by galaxies of type ≥ Scd (78%), whose distance has been determined using $H_0 = 73$ km s^{-1} Mpc^{-1}, the average HI−def is only marginally affected by the choice of $H_0 = 100$ km s^{-1} Mpc^{-1} for Sa-Sc galaxies of Solanes et al. (1996). The rest of the difference (0.18 in HI−def) might be due to statistical reasons, our sample (55 objects) being more than twice the size of that of Garcia-Barreto et al. (1994) (23 objects), or to the adopted calibration. Garcia-Barreto et al. (1994) determined the HI-deficiency parameter using the *B* band luminosity relation of Giovanelli et al. (1981), while our estimate is based on a diameter relation. The calibration of the HI-deficiency on optical diameters is less dispersed than that based on optical luminosities (Haynes & Giovanelli 1984).

We can thus conclude that late-type galaxies in the Coma I cloud are not as deficient in HI gas as previously claimed. The Coma I cloud is thus composed of galaxies with a similar spiral fraction but richer in gas content than the Virgo M and W clouds. Being at a distance along the line of sight similar to that of Virgo (14.52 Mpc for Coma I and 16.5 Mpc for Virgo), and at a distance of ∼5 Mpc on the plane of the sky to the core of the cluster, it could be considered as a cloud of Virgo (for comparison the M and W clouds are located at ∼16 Mpc from the core of Virgo, Gavazzi et al. 1999). Is pre-processing acting on the late-type galaxy population in the Coma I cloud? From a statistical point of view, the present analysis excludes it. There exists, however, a fraction of objects with a significant HI-deficiency (HI−def > 0.3). What is its origin? Because of the relatively poor statistics and the low density contrast within the cloud, it is impossible to disentangle gravitational interactions from interactions with the intergalactic medium within the Coma I cloud itself or during the crossing of the whole cloud through the core of the Virgo cluster. The spread of the HI-deficient galaxies (HI−def > 0.3) within the cloud and in the velocity-distance space (Fig. 4) do not seem to favor the former scenario, since gravitational interactions or ram-pressure stripping within the cloud would be more efficient in the highest density regions or for galaxies with the highest velocities with respect to the mean value of the Coma I cloud. Indeed using the prescription of Boselli & Gavazzi (2006) we can estimate that the frequency of galaxy encounters within the Coma I cloud is very low, the relaxation time being ∼40 Gyr. Despite the process in place, however, if the Coma I cloud is representative of infalling groups in nearby clusters, we conclude that in the nearby universe the gas properties of late-type galaxies belonging to large substractures of rich clusters do not appear significantly perturbed by their environment. The ongoing ALFALFA survey (Giovanelli et al. 2005) will soon provide us with an unprecedent sky coverage in HI of 7000 sq. degrees of the sky, thus covering a large range in galaxy density from the core of rich clusters to the local voids. In particular, given its sensitivity (2.4 mJy at 5 km s^{-1}, Giovanelli et al. 2005) combined with a multi-beam detector, ALFALFA will be perfectly suited for observing at the same time extended sources and point-like objects as those populating the Coma I cloud. This survey will thus be a unique opportunity for studying, using a homogenous dataset and with an unprecedent statistical significance, the gas properties of galaxies in different density regimes of the local universe, including loose groups and substructures probably infalling into rich clusters.

Acknowledgements. We want to thank C. Marinoni, L. Cortese, C. Pacifici and S. Boissier for interesting discussions, and the anonymous referee for useful comments. This research has made use of the NASA/IPAC Extragalactic Database (NED) which is operated by the Jet Propulsion Laboratory, California Institute of Technology, under contract with the National Aeronautics and Space Administration. We acknowledge the usage of the HyperLeda database (http://leda.univ-lyon1.fr) and the GOLDMine database (http://goldmine.mib.infn.it/).

References

Boselli, A., & Gavazzi, G. 2006, PASP, 118, 517
Boselli, A., Gavazzi, G., Donas, J., & Scodeggio, M. 2001, AJ, 121, 753
Burstein, D., Krumm, N., & Salpeter, E. 1987, AJ, 94, 883
Chamaraux, P., Balkowski, C., & Fontanelli, P. 1987, A&AS, 69, 263
Cortese, L., Gavazzi, G., Boselli, A., Iglesias-Paramo, J., & Carrasco, L. 2004, A&A, 425, 429
Cortese, L., Gavazzi, G., Boselli, A., et al. 2006, A&A, 453, 847
Dahlem, M., Ehle, M., Ryder, S., Vlajic, M., & Haynes, R. 2005, A&A, 432, 475
Donnelly, R., Forman, W., Jones, C., et al. 2001, ApJ, 562, 254
Dressler, A. 1980, 236, 351
Dressler, A. 2004, in Clusters of Galaxies: Probes of Cosmological Structure and Galaxy Evolution, from the Carnegie Observatories Centennial Symposia, Published by Cambridge University Press, as part of the Carnegie Observatories Astrophysics Series, ed. J. S. Mulchaey, A. Dressler, & A. Oemler, 206
Ferrarese, L., Mould, J., Kennicutt, R., et al. 2000, ApJ, 529, 745
Ferrari, C., Maurogordato, S., Cappi, A., & Benoist, C. 2003, A&A, 399, 813
Fisher, J. R., & Tully, B. 1981, ApJS, 47, 139
Garcia-Barreto, J. A., Downes, D., & Huchtmeier, W. 1994, A&A, 288, 705
Gavazzi, G., & Boselli, A. 1996, Astro. Lett. Commun., 35, 1
Gavazzi, G., Boselli, A., Scodeggio, M., Pierini, D., & Belsole, E. 1999, MNRAS, 304, 595
Gavazzi, G., Boselli, A., Pedotti, P., Gallazzi, A., & Carrasco, L. 2002, A&A, 396, 449
Gavazzi, G., Cortese, L., Boselli, A., et al. 2003a, ApJ, 597, 210
Gavazzi, G., Boselli, A., Donati, A., Franzetti, P., & Scodeggio, M. 2003b, A&A, 400, 451
Gavazzi, G., Boselli, A., van Driel, W., & O'Neil, K. 2005, A&A, 429, 439
Gavazzi, G., Boselli, A., Cortese, L., et al. 2006a, A&A, 446, 839

Gavazzi, G., O'Neil, K., Boselli, A., & van Driel, W. 2006b, A&A, 449, 929
Gavazzi, G., Giovanelli, R., Haynes, M., et al. 2008, A&A, 482, 43
Giovanelli, R., Chincarini, G., & Haynes, M. 1981, ApJ, 247, 383
Giovanelli, R., Haynes, M., Kent, B., et al. 2005, AJ, 130, 2598
Gnedin, O. 2003, ApJ, 582, 141
Gomez, P., Nichol, R., Miller, C., et al. 2003, ApJ, 584, 210
Gregory, S., & Thompson, Li. 1977, ApJ, 213, 345
Jarrett, T., Chester, T., Cutri, R., Schneider, S., & Huchra, J. 2003, AJ, 125, 525
Haynes, M., & Giovanelli, R. 1984, AJ, 89, 758
Helou, G., Hoffman, G., & Salpeter, E. 1984, ApJS, 55, 433
Huchtmeier, W. 1982, A&A, 110, 121
Huchtmeier, W., & Richter, O. 1989, in A General Catalog of HI Observations of Galaxies (Springer-Verlag)
Huchtmeier, W., Krishna, G., & Petrosian, A. 2005, A&A, 434, 887
Lewis, B. M. 1987, ApJS, 63, 515
Lewis, I., Balogh, M., De Propris, R., et al. 2002, MNRAS, 334, 673
Masters, K., Springob, C., & Huchra, J. 2008, AJ, 135, 1738
Noordermeer, E., van der Hulst, J., Sancisi, R., Swaters, R., & van Albada, T. 2005, A&A, 442, 137
Rots, A. 1980, A&AS, 41, 189
Sakai, S., Kennicutt, R., van der Hulst, J., & Moss, K. 2002, ApJ, 578, 842
Schneider, S., Thuan, T., Magri, C., & Wadjak, J. 1990, ApJS, 72, 245
Scodeggio, M., & Gavazzi, G. 1993, ApJ, 409, 110
Springob, C., Haynes, M., Giovanelli, R., & Kent, B. 2005, ApJS, 160, 149
Solnes, J., Giovanelli, R., & Haynes, M. 1996, ApJ, 461, 609
Theureau, G., Bottinelli, L., Coudreau, N., et al. 1998, A&AS, 130, 333
Thuan, T. 1981, ApJ, 247, 823
Tully, B. 1988a, AJ, 96, 73
Tully, B. 1988b, Nearby Galaxy Catalog (Cambridge University Press)
Whitmore, B., & Gilmore, D. 1991, ApJ, 367, 64